ASTRA

Astrophysics and Space Sciences
Transactions

The cosmic ray energy spectrum in the range $10^{16} - 10^{18}$ eV measured by KASCADE-Grande

M. Bertaina[3], W.D. Apel[1], J.C. Arteaga-Velázquez[2,a], K. Bekk[1], J. Blümer[1,2], H. Bozdog[1], I.M. Brancus[4], P. Buchholz[5], E. Cantoni[6,3,1], A. Chiavassa[3], F. Cossavella[2,b], K. Daumiller[1], V. de Souza[2,c], F. Di Pierro[3], P. Doll[1], R. Engel[1], J. Engler[1], M. Finger[1], D. Fuhrmann[7], P.L. Ghia[6], H.J. Gils[1], R. Glasstetter[7], C. Grupen[5], A. Haungs[1], D. Heck[1], J.R. Hörandel[2,d], T. Huege[1], P.G. Isar[1], K.-H. Kampert[7], D. Kang[2], D. Kickelbick[5], H.O. Klages[1], K. Link[2], P. Łuczak[8], M. Ludwig[2], H.J. Mathes[1], H.J. Mayer[1], M. Melissas[2], J. Milke[1], B. Mitrica[4], C. Morello[6], G. Navarra[3,e], S. Nehls[1], J. Oehlschläger[1], S. Ostapchenko[1,f], S. Over[5], N. Palmieri[2], M. Petcu[4], T. Pierog[1], H. Rebel[1], M. Roth[1], H. Schieler[1], F. Schröder[1], O. Sima[9], G. Toma[4], G.C. Trinchero[6], H. Ulrich[1], A. Weindl[1], J. Wochele[1], M. Wommer[1], and J. Zabierowski[8]

[1]Institut für Kernphysik, Karlsruher Institut für Technologie - Campus Nord, Germany
[2]Institut für Experimentelle Kernphysik, Karlsruher Institut für Technologie - Campus Süd, Germany
[3]Dipartimento di Fisica Generale dell' Università, Torino, Italy
[4]National Institute of Physics and Nuclear Engineering, Bucharest, Romania
[5]Fachbereich Physik, Universität Siegen, Germany
[6]Istituto di Fisica dello Spazio Interplanetario, INAF Torino, Italy
[7]Fachbereich Physik, Universität Wuppertal, Germany
[8]Soltan Institute for Nuclear Studies, Lodz, Poland
[9]Department of Physics, University of Bucharest, Bucharest, Romania
[a]now at: Universidad Michoacana, Instituto de Física y Matemáticas, Mexico
[b]now at: Max-Planck-Institut für Physik, München, Germany
[c]now at: Universidade São Paulo, Instituto de Física de São Carlos, Brasil
[d]now at: Dept. of Astrophysics, Radboud University Nijmegen, The Netherlands
[e]deceased
[f]now at: University of Trondheim, Norway

Abstract. The KASCADE-Grande experiment, located at Campus North of the Karlsruhe Institute of Technology (Germany) is a multi-component extensive air-shower experiment devoted to the study of cosmic rays and their interactions at primary energies $10^{14} - 10^{18}$ eV. One of the main goals of the experiment is the measurement of the all particle energy spectrum in the $10^{16} - 10^{18}$ eV range, i.e. extending the range accessible by KASCADE alone. The Grande detector samples the charged component (N_{ch}) of the air shower while the original KASCADE array provides in addition a measurement of the muon component (N_μ). The combined information of N_{ch} and N_μ is used to estimate the energy on an event-by-event basis and to derive the all-particle energy spectrum. Since the calibration of the observables in terms of the primary energy depends on Monte Carlo simulations, three different methods with partially different sources of un-certainties, have been considered and compared to each other to derive the systematics on the energy spectrum. The different methods employed to derive the spectrum and their uncertainties, as well as the implications of the obtained result, are discussed in detail.

1 Introduction

The study of the energy spectrum and of the chemical composition of cosmic rays are fundamental tools to understand origin, acceleration and propagation of cosmic rays. The range between 10^{16} eV and 10^{18} eV can only be studied by means of air-shower arrays which sample specific components of the cascade of particles produced by the primary cosmic ray in the atmosphere. This range is quite important from astrophysical point of view because it is expected that in this energy range the transition between galactic and extragalactic origin of cosmic rays will occur. The results obtained at lower energies by KASCADE (Antoni et al., 2005)

and EAS-TOP (Aglietta et al., 2004) as well as by other experiments suggest that the knee in the primary energy spectrum around $3 - 4 \times 10^{15}$ eV is due to the break in the spectra of light elements. Moreover, KASCADE results seem to indicate that a rigidity dependent mechanism is responsible for such knees. Therefore, a knee of the heaviest components would be expected in the range of 10^{16} eV to 10^{18} eV. Various theories with different assumptions try to explain the rather smooth behavior of the cosmic ray energy spectrum between 10^{16} eV and 10^{18} eV. The idea of the "dip model" (Berezinsky et al., 2006) is that the ankle at $(4 - 10) \cdot 10^{18}$ marks the energy loss by electron pair production of extragalactic protons, hence, at these energies the composition is already proton dominant and the transition between galactic and extra-galactic components already happens at energies lower than 10^{18} eV. On the other hand, Hillas (Hillas, 2005) proposed the idea of a "component B" of cosmic rays of galactic origin which shows a rigidity dependence, like the "component A" responsible for the well-known knee, but shifted in energy. In this case, the transition between galactic and extragalactic components will occur at the ankle, and in the region between 10^{16} eV and 10^{18} eV a mixed composition is expected to prevail.

In order to discriminate between the different models, a very precise measurement of the possible structures of the energy spectrum is needed. The aim of the KASCADE-Grande experiment is to provide high-quality data in exactly this energy range by using the sizes of the charged-particle and muon components.

2   The apparatus

The KASCADE-Grande experiment (Apel et al., 2010) is a multi-detector setup consisting of the KASCADE experiment (Antoni et al., 2003), the trigger array Piccolo and the scintillator detector array Grande. Additionally, KASCADE-Grande includes an array of digital read-out antennas, LOPES (Falcke et al., 2005; Schröder et al., 2011), to study the radio emission in air showers at $E > 10^{17}$ eV. Most important for the analysis presented here are the two scintillator arrays: KASCADE and Grande. The KASCADE array comprises 252 scintillator detector stations structured in 16 clusters. The detector stations house two separate detectors for the electromagnetic (unshielded liquid scintillators) and muonic components (shielded plastic scintillators) where muon detectors are housed in 12 clusters (or 192 stations), only. This enables to reconstruct the lateral distributions of muons and electrons separately on an event-by-event basis. The Grande array is formed by 37 stations of plastic scintillator detectors, $10\,\mathrm{m}^2$ each (divided into 16 individual scintillators) spread on a $0.5\,\mathrm{km}^2$ surface, with an average grid size of $137\,\mathrm{m}$. All the 16 scintillators per station are viewed by a high gain photomultiplier (for timing and low particle density measurements) and the four central ones are

additionally viewed by a low gain one (for high particle densities). The dynamic range of the detectors is $0.3 - 8000$ particles / $10\,\mathrm{m}^2$. Grande is arranged in 18 hexagonal clusters formed by 6 external detectors and a central one. Grande and KASCADE arrays are both triggered when all the 7/7 stations in a hexagon have fired (rate $\sim 0.5\,\mathrm{Hz}$). Full efficiency for proton and iron primaries is reached at $\log N_{ch} > 5.8$.

KASCADE-Grande provides the unique opportunity of evaluating the reconstruction accuracies of the Grande array by a direct comparison with an independent experiment. For a subsample of events collected by the Grande array it is possible to compare on an event-by-event basis the two independent reconstructions of KASCADE and Grande. By means of such a comparison the Grande reconstruction accuracies are found to be for the shower size: systematic uncertainty $\leq 5\%$, statistical inaccuracy $\leq 15\%$; for arrival direction: $\sigma \approx 0.8°$; for the core position: $\sigma \approx 6\,\mathrm{m}$ (Apel et al., 2010). All of them are in good accordance with the resolutions obtained from simulations.

3   The analysis

A sample of Monte Carlo data was simulated including the full air shower development in the atmosphere, the response of the detector and its electronics as well as their uncertainties. In this way, the reconstructed parameters from simulation are obtained in the same way as for real data. The EAS events were generated with an isotropic distribution with spectral index $\gamma = -3$ and were simulated with CORSIKA (Heck et al., 1998) and the hadronic Monte Carlo generators FLUKA (Fassò et al., 2005) and QGSJet II (Ostapchenko, 2006a,b). Sets of simulated events were produced in the energy range from 10^{15} eV to 10^{18} eV with high statistics and for five different representative mass groups: H, He, C, Si and Fe (≈ 353.000 events per primary). Few events up to $3 \cdot 10^{18}$ eV were also generated in order to cross-check the reconstruction behavior at the highest energies.

Grande stations are used to provide core position and angle-of-incidence as well as the total number of charged particles in the shower, by means of a maximum likelihood procedure comparing the measured number of particles with the one expected from a modified NKG lateral distribution function (Apel et al., 2006) of charged particles in the EAS.

The total number of muons is calculated using the core position determined by the Grande array and the muon densities measured by the KASCADE muon array detectors. The total number of muons N_μ in the shower disk (above the energy threshold of $230\,\mathrm{MeV}$) is derived from a maximum likelihood estimation assuming the locally detected muons to fluctuate according to a Poisson distribution. Here, we have chosen a lateral distribution function based on the one proposed by Lagutin and Raikin (Lagutin and Raikin, 2001). Since the muon densities are very low, except for the highest energy showers, stable fits on shower-by-shower basis are

only obtained if the shape of the lateral distribution function is kept constant and only the muon number N_μ is taken as a free parameter. By means of Monte Carlo simulations a resolution of the total muon number in the showers of $\approx 25\%$ for energies above 10^{16} eV is expected. The reconstruction procedures and obtained accuracies of KASCADE-Grande observables are described in detail in Apel et al. (2010).

For the reconstructed events, we restricted ourselves to events with zenith angles lower than $40°$ due to increasing muon number and shower size uncertainties coming from the reconstruction procedure. Additionally, only air showers with cores located in a central area on KASCADE-Grande, represented in Fig. 1, were selected. With this cut on the fiducial area, border effects are discarded and the under- and overestimations of the muon number for events close to and far away from the center of the KASCADE array are reduced. This is motivated by the fact that the muon detector is asymmetrically located with respect to the array. Therefore, in case of small and large distances, the total number of muons obtained by fitting the local muon densities with the lateral distribution function in a limited range of distances, would introduce some bias for very small and large core distances. All of these cuts were applied also to the Monte Carlo simulations to study the effects and to optimize the cuts. Full efficiency for triggering and reconstruction of air-showers is reached at primary energy of $\approx 10^{16}$ eV, slightly depending on the cuts needed for the reconstruction of the different observables (Apel et al., 2010).

The analysis presented here is finally based on 1173 days of data and the cuts on the sensitive central area and zenith angle correspond to a total acceptance of $A = 1.976 \cdot 10^9$ cm^2 sr, and an exposure of $N = 2.003 \cdot 10^{17}$ cm^2 s sr.
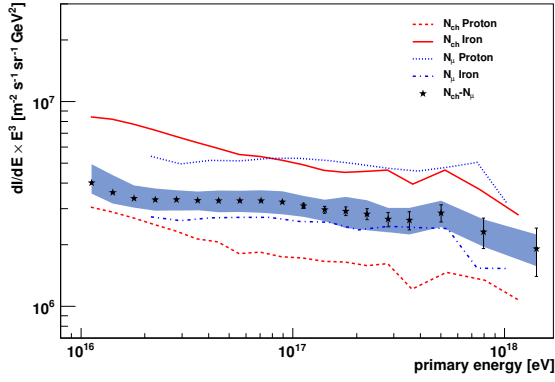
In KASCADE-Grande, the all-particle energy spectrum is derived by means of different techniques: using only one component, such as the size of the charged (Kang et al., 2009) or muon (Arteaga et al., 2009) components, a combination of the two (Bertaina et al., 2009), or the particle density at 500 m, S(500) (Toma et al., 2009). In this way, by combining and comparing the results of the different methods, which are sensitive to different parameters of the showers, and have intrinsically partially different systematics or sources of uncertainty it is possible to: (i) cross-check the measurements by different sub-detectors; (ii) cross-check the reconstruction procedures; (iii) cross-check the influence of systematic uncertainties; (iv) test the sensitivity of the observables to the elemental composition; (v) test the validity of hadronic interaction models underlying the simulations.

The conversion between the observed quantities (charged particle and muon sizes as well as the combination of both) of the EAS to the energy of the primary particle requires the assumption of a specific hadronic interaction model, whose general suitability has to be verified beforehand. In this work, the energy estimations are based on the CORSIKA-QGSjetII model, motivated by the fact that this model reproduces fairly well the distributions of the ratio of the muon and electron
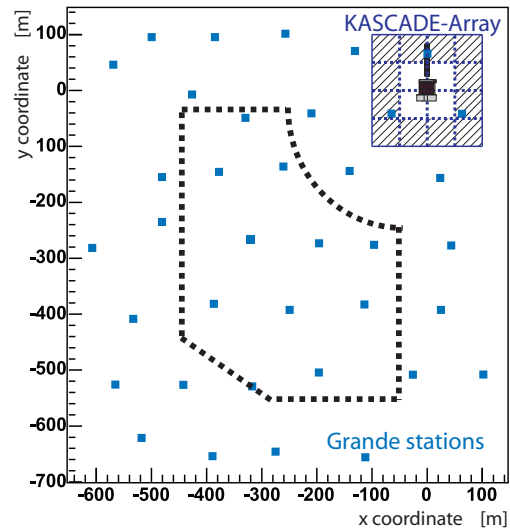
Fig. 1. Layout of the KASCADE-Grande experiment: The original KASCADE and the distribution of the 37 stations of the Grande array are shown. The outer 12 clusters of the KASCADE array employ also shielded μ-detectors. The dashed line shows the area used in the present analysis.

sizes measured by KASCADE-Grande as a function of both, the electron size and the atmospheric depth (up to $40°$ zenith angle) (Cantoni et al., 2009). In the following, results will be presented on the basis of three among these methods: N_{ch} or N_μ alone and their combination. In the N_{ch}-method and N_μ-method, the reconstructed charged particle or muon shower size per individual event is corrected for attenuation in the atmosphere by the constant intensity cut method and calibrated by Monte Carlo simulations under the assumption of a dependence $E_0 \propto N_{ch}^{\alpha_{ch}}$ ($E_0 \propto N_\mu^{\alpha_\mu}$) and a particular primary composition (Kang et al., 2009; Arteaga et al., 2009). The energy conversion relation (calibration function) is obtained by selecting events of zenith angle ranges of $17° \leq \theta \leq 24°$, i.e. around the reference angle ($20°$ for N_{ch} and $22°$ for N_μ distributions), to reduce systematic effects. The relation of the primary energy as a function of the number of charged particles (muons) is obtained assuming a linear dependence in logarithmic scale $\log E_0 = a_{N_{ch,\mu}} + b_{N_{ch,\mu}} \cdot \log N_{ch,\mu}$. The same procedure is performed for H, He, C, Si and Fe primaries as well as for a uniform mixed composition to examine the dependence of the calibration on the assumed primary particle type. The energy resolution is estimated from the difference between simulated and derived energy. In case of N_{ch} (N_μ) the energy resolution for proton and iron are about 31% (25%) and 15% (12%), respectively, over the whole energy ranges, where the reconstruction uncertainty for N_{ch} gives the largest contribution. In addition, the systematic uncertainties on the reconstructed energy spectrum are investigated considering various possible contributions: a) the associated errors to the fit of the attenuation curve and of the calibration function, b) uncertainties due to a possible misdescription of the attenuation in the Monte Carlo simulation

Fig. 2. Reconstructed all-particle energy spectrum by the three different methods applied to KASCADE-Grande data. For the $N_{ch} - N_\mu$ method a band is shown indicating the range of the systematic uncertainty.

are estimated by using two different reference zenith angles (10 and 30 degrees), c) shower fluctuations, d) uncertainty in the spectral index. All these individual systematic contributions were considered to be uncorrelated, and combined thus in quadrature to obtain the total systematic uncertainty, where the composition dependence was not taken into account. The systematic uncertainty (i.e. sum in quadrature of all terms discussed above except the energy resolution) on the flux for proton and iron are for N_{ch} (N_μ) 21% (7%) and 17% (13%), respectively, at energies of 10^{17} eV. Finally, to reduce the effects of the fluctuations on the determined energy spectrum, an unfolding procedure is applied which uses a response matrix built using Monte Carlo simulations. This matrix represents the probability that an event being reconstructed with an energy inside the bin $\log_{10}(E_i)$ has a true energy in the channel $\log_{10}(E_j^{True})$. By unfolding such matrix it is possible to deconvolve the effect of shower fluctuations.

In the $N_{ch} - N_\mu$ method, the information provided by the two observables is combined. By help of Monte Carlo simulations a formula is obtained to calculate the primary energy per individual shower on the basis of N_{ch} and N_μ. The formula takes into account the mass sensitivity in order to minimize the composition dependence. Advantage of this technique is that the correlation between the two particle components is taken into account on an event-by-event basis. The attenuation is corrected for by deriving the formula for different zenith angle intervals independently and combining the energy spectrum afterwards (Bertaina et al., 2009). The energy assignment is defined as $E = f(N_{ch}, k)$ (see Eq. (1)), where N_{ch} is the size of the charged particle component and the parameter k is defined through the ratio of the sizes of the N_{ch} and muon (N_μ) components: $k = g(N_{ch}, N_\mu)$ (see Eq. (2)). The main aim of the k variable is to take into account the average differences in the N_{ch}/N_μ ratio among different primaries with same N_{ch} and the shower to shower fluctuations for events of the same primary mass:

$$\log_{10}(E[GeV]) = [a_p + (a_{Fe} - a_p) \cdot k] \cdot \log_{10}(N_{ch})$$

$$+ b_p + (b_{Fe} - b_p) \cdot k \tag{1}$$

$$k = \frac{\log_{10}(N_{ch}/N_\mu) - \log_{10}(N_{ch}/N_\mu)_p}{\log_{10}(N_{ch}/N_\mu)_{Fe} - \log_{10}(N_{ch}/N_\mu)_p} \tag{2}$$

$$\log_{10}(N_{ch}/N_\mu)_{p,Fe} = c_{p,Fe} \cdot \log_{10}(N_{ch}) + d_{p,Fe}. \tag{3}$$

The k parameter is, by definition of Eq. (2), a number centered around 0 for a typical proton shower and 1 for a typical iron shower. Also in this case a response matrix is applied afterwards to take into account the migration of low energy events to higher energies. After applying the procedure to the 5 angular bins independently, a combined spectrum is obtained by using all the events of the 5 bins calibrated with their own calibration function. Also in this case systematic uncertainties due to the following reasons were considered: a) different intensity in the five angular bins, b) capability of reproducing an, a priori assumed, single primary spectrum with slope $\gamma = -3$, c) uncertainty on the index of the energy spectrum used to derive the energy relation $E(N_{ch})$ and the response matrix, d) uncertainty on the core location. The total uncertainty is around 15% and it is quite stable in the entire energy range. Regarding the energy resolution, it varies between 26% at the threshold and 20% at the highest energies due to the decrease of the intrinsic shower fluctuations.

4   Results

In Fig. 2 the resulting spectra are compiled, where the flux is multiplied by a factor of $E^{3.0}$. Owing to the different procedures, the results for the first two methods are shown under proton and iron assumption, respectively, only, whereas for the other method the resulting all-particle energy spectrum is displayed with a band for systematic uncertainties. Taking into account the systematic uncertainties, there is a fair agreement between the all-particle energy spectra of the different applications.

Of particular interest is the fact that by using N_{ch}, the iron assumption predicts a higher flux than the proton assumption, whereas using N_μ the opposite is the case. That means that the "true" spectrum has to be a solution inside the range spanned by the two methods. If there is only the possibility of applying one method, then there is a large variance in possible solutions (everything within the range spanned by proton and iron line, not even parallel to these lines). However, more detailed investigations have shown, that a structure in the spectrum or a sudden change in composition would be retained in the resulting spectrum, even if the calibration is performed with an individual primary, only. All variations (within reasonable physics scenarios, i.e. everything between pure proton and pure iron, including other mass groups) of the composition would lead to a spectrum within the given error band. Interestingly, over the whole energy range there is only little room for a solution satisfying both ranges, spanned by N_{ch} and N_μ, and this solution

has to be of relatively heavy composition - in the framework of the QGSJet-II hadronic interaction model. The narrower range for a solution provided by the N_μ method compared to N_{ch} confirms the finding of KASCADE that at sea-level the number of mostly low-energy muons N_μ is a very good and composition insensitive energy estimator. The results of the composition independent N_{ch}-N_μ method lie inside the area spanned by the composition dependent methods, again confirming that the reconstructions of the shower size are under control. In addition, this finding expresses a cross-check of the intrinsic consistency of the hadronic interaction model. Future investigations will perform a similar analysis to test the validity of the interaction model EPOS (Werner et al., 2006) to describe the air shower development.

Despite the overall very smooth power law behavior of the resulting all-particle spectrum, there are some smaller structures observed, which does not allow to describe the spectrum with a single slope index. Figure 3 shows the resulting all-particle energy spectrum multiplied with a factor that the middle part of the spectrum is flat. There is a clear evidence that just above 10^{16} eV the spectrum shows a "concave" behavior, which is significant with respect to the systematic and statistical uncertainties. Such a hardening of the spectrum is expected when a pure rigidity dependence of the galactic cosmic rays is assumed. In this case the gap between light primaries (proton, helium) and the CNO ($Z = 6 - 12$) group in their knee positions requires a hardening of the spectrum (De Donato and Medina, 2009). But there are also other astrophysical scenarios possible for a concave behavior of the cosmic ray spectrum. In general, a transition from one source population to another one should result in a hardening of the spectrum. In this aspect, the KASCADE-Grande result could be a first experimental hint to the "component B" of galactic cosmic rays as proposed by Hillas (2005). Another feature visible in the spectrum is a small break at around 10^{17} eV. A fit with a power law spectrum above 10^{17} eV gives a spectral index of $\gamma = -3.24 \pm 0.08$. A preliminary statistical analysis with the F-test shows that the significance associated with this change of the spectral index is at the level of 99.8%. It is noteworthy that a somewhat different spectral feature at $50 - 80$ PeV has been reported by the GAMMA experiment (Garyaka et al., 2008), which rather observed a "bump" instead of the spectral break seen by KASCADE-Grande.

5   Conclusions

Figure 4 shows the all-particle energy spectrum together with the results of other experiments. At the threshold, there is a good overlap with the results obtained by KASCADE and EAS-TOP. This is somehow expected as the analysis performed on the subsample of events reconstructed by both, KASCADE and KASCADE-Grande, showed no significant systematical effects. The spectrum doesn't follow a pure power-law on the entire energy range. The features observed around few 10^{16} eV and close to 10^{17} could give interest-
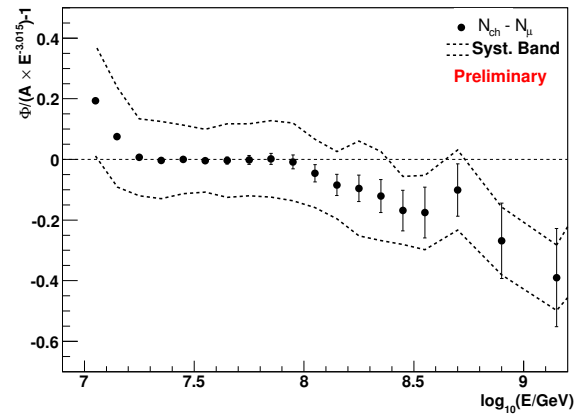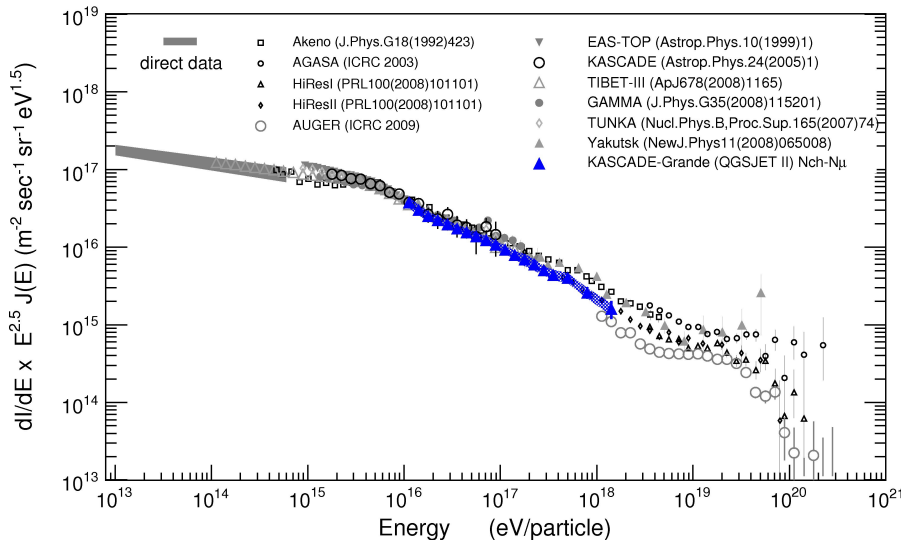

Fig. 3. Residual plot for the reconstructed all-particle energy spectrum obtained from KASCADE-Grande through the $N_{ch} - N_\mu$ method. The systematic error band is also shown (dotted lines).

ing hints to the astrophysical processes in the transition region from galactic to extragalactic origin of cosmic rays. As the change of spectral index is small compared to the main knee, a significant conclusion is not possible without investigating the composition in detail in this energy range. These composition studies are presently underway at KASCADE-Grande adopting different approaches based on N_{ch} and N_μ observables, among them: a) the reconstruction of the local muon densities at a certain distance to the shower core as it gives a sensitivity to changes in the elemental composition (De Souza et al., 2009); b) the electron/muon number ratio (Cantoni et al., 2009); c) the evolution of the variable k as defined in Eq. (2); d) an unfolding procedure, similar to what was already performed with the KASCADE data (Antoni et al., 2005). Finally, at the highest energies, the spectrum quite naturally overlaps, inside the statistical and systematic uncertainties, with Hi-Res (Abbasi et al., 2008) and Auger (Schüssler, 2009) results.

Fig. 4. Comparison of the all-particle energy spectrum obtained with KASCADE-Grande data to results of other experiments. The band around the KASCADE-Grande spectrum denotes the systematic uncertainties in the flux estimation.

References

Abbasi, R U et al. (Hi-Res Coll.): First Observation of the GZK Suppression, Phys. Rev. Lett., 100, 101101, 2008.

Aglietta, M. et al. (EAS-TOP Coll.): The CR primary composition in the "knee" region through the EAS electromagnetic and muon measurements at EAS-TOP, Astrop. Phys., 21, 583, 2004.

Antoni, T. et al. (KASCADE Coll.): The cosmic-ray experiment KASCADE, NIM A 513, 490, 2003.

Antoni, T. et al. (KASCADE Coll.): KASCADE measurements of energy spectra for elemental groups of cosmic rays: Results and open problems, Astrop. Phys., 24, 1, 2005.

Apel, W. D. et al. (KASCADE Coll.): Comparison of measured and simulated lateral distributions for electrons and muons with KASCADE, Astrop. Phys., 24, 467, 2006.

Apel, W. D. et al. (KASCADE-Grande Coll.): The KASCADE-Grande experiment, NIM A 620, 202 (2010).

Arteaga, J. C. et al. (KASCADE-Grande Coll.): The Energy Spectrum of Primary Cosmic Rays Reconstructed with the KASCADE-Grande Muon Data, in: Proc. 31th ICRC, Lodz (Poland), #icrc0805, 2009.

Berezinsky, V., Gazizov, A., and Grigorieva, S.: On astrophysical solution to ultrahigh energy CR, Phys. Rev. D 74 043005, 2006.

Bertaina, M. et al. (KASCADE-Grande Coll.): The all particle energy spectrum of KASCADE-Grande in the energy region 10^{16} - 10^{18} eV by means of the N_{ch} - N_μ technique, in: Proc. 31th ICRC, Lodz (Poland), #icrc0323, 2009.

Cantoni, E. et al. (KASCADE-Grande Coll.): The sensitivity of KASCADE-Grande to the cosmic ray primary composition between 10^{16} and 10^{18} eV, in: Proc. 31th ICRC, Lodz (Poland), #icrc0524, 2009.

De Donato, C. and Medina-Tanco, G.A.: Experimental constraints on the astrophysical interpretation of the cosmic ray Galactic-extragalactic transition region, Astrop. Phys., 32, 253, 2009.

De Souza, V. et al. (KASCADE-Grande Coll.): A direct measurement of the muon component of air showers by the KASCADE-Grande Experiment, in: Proc. 31th ICRC, Lodz (Poland), #icrc0499, 2009.

Falcke, H. et al. (LOPES Coll.): Detection and imaging of atmosph. radio flashes from CR air showers, Nature 435, 313, 2005.

Fassò, A. et al.: FLUKA: A multi-particle transport code, Report CERN-2005-10, INFN/TC-05/11, SLAC-R-773, 2005.

Garyaka, A P. et al. (GAMMA Coll.): An all-particle primary energy spectrum in the 3-200 PeV energy range, J. Phys. G, 35, 115201, 2008.

Heck, D., Knapp, J., Capdevielle, J. N. et al.: A Monte Carlo Code to Simulate Extensive Air Showers, Report FZKA 6019, Forschungszentrum Karlsruhe, 1998.

Hillas, A. M.: Can diffusive shock acceleration in supernova remnants account for high-energy galactic cosmic rays?, J. Phys. G: Nucl. Part. Phys., 31, 95, 2005.

Kang, D. et al. (KASCADE-Grande Coll.): Cosmic ray energy spectrum based on shower size measurements of KASCADE-Grande, in: Proc. 31th ICRC, Lodz (Poland), #icrc1044, 2009.

Lagutin, A. A. and Raikin, R. I.: Lateral distribution of electrons in EAS at superhigh energies: predictions and experimental data, Nucl. Phys. Proc. Suppl., 97, 274, 2001.

Ostapchenko, S. S.: QGSJET-II: towards reliable description of very high energy hadronic interactions, Nucl. Phys. B (Proc. Suppl.) 151, 143 and 147, 2006a;

Ostapchenko, S. S.: Nonlinear screening effects in high energy hadronic interactions, Phys. Rev. D 74, 014026, 2006b.

Schröder, F. et al. (LOPES Coll.): Measurement of Cosmic Ray Air Showers with the Digital Radio Interferometer LOPES, ASTRA, this spec. issue, 2011.

Schüssler, F. et al. (Auger Coll.): Measurement of the cosmic ray energy spectrum above 10^{18} eV with the Pierre Auger Observatory, in: Proc. 31th ICRC, Lodz (Poland), #icrc0114, 2009.

Toma, G. et al. (KASCADE-Grande Coll.): Primary energy reconstruction from the S(500) observable recorded with the KASCADE-Grande detector array, in: Proc. 31th ICRC, Lodz (Poland), #icrc0347, 2009.

Werner, K., Liu, F. M., and Pierog, T.: Parton ladder splitting and the rapidity dependence of transverse momentum spectra in deuteron-gold collisions at the BNL Relativistic Heavy Ion Collider, Phys. Rev. C, 74, 044902, 2006.